International Journal of Minerals, Metallurgy and Materials
Accepted manuscript, https://doi.org/10.1007/s12613-019-1899-1
© University of Science and Technology Beijing and Springer-Verlag GmbH Germany, part of Springer Nature 2020

Reinforcing Effect of Laminate Structure on the Fracture Toughness of Al_3Ti Intermetallic

Yang Cao[1)], *Dan-dan Zhang*[1)], *Pei-jun Zhou*[2)], *Kun Liu*[1)], *Wuyi Ming*[1)] and *Jun Ma*[1),*]

1) Mechanical and Electrical Engineering Institute, Zhengzhou University of Light Industry, Zhengzhou 450002, China

2)Key Laboratory of Superlight Materials & Surface Technology Ministry of Education，Harbin Engineering University, Harbin 150001, China

Abstract: Metal/intermetallic laminate composites can improve the mechanical properties of intermetallic materials using metal layers. In this study, Ti/Al_3Ti laminate composite is synthesized from titanium and aluminum foils using vacuum hot-pressed sintering technology. The microstructure of the prepared material is analyzed by SEM and EBSD. Results illustrate that both Ti and Al_3Ti are single phase and there is obvious stress concentration on the interface. To obtain indentation and cracks, loads are applied to different locations of the composite by microhardness tester. The growth path of the cracks is then observed under microscope, showing that crack propagation is prevented by the interface between Ti and Al_3Ti layers, and the cracks which propagated parallel to the laminate are shifted to the interface. The fracture toughness for different areas, including Al_3Ti layers, interface, and near-interface zone, are measured by indentation fracture method. The fracture toughness at and near the interface is 1.7 and twice that of the Al_3Ti layers, respectively. Results indicate that crack blunting and crack front convolution by the laminate structure is primarily responsible for increased toughness.

Keywords: Interface; Al_3Ti compound; Ti/Al_3Ti laminate composite; toughening effect; indentation fracture method

1. Introduction

Laminate structures are used to improve the strength and toughness of many materials including intermetallic, titanium alloy and steel. Lamellar composite materials are formed by interlayer bonding of different materials and have numerous application potentials. A number of metal laminates such as Ti-Al [1,2], Ni-Al [3,4], Nb-Al [5,6], Ti-Cu [7,8], and Ti-TiBw/Ti [9] composites have been previously prepared. Research indicates that composites are effectively improved by incorporating ductile reinforcements layers using various toughing mechanisms including weak interfaces, crack bridging, ductile ligament, multiple cracking, crack bifurcation, and crack deflection.

In the enhancement of stainless steel and multilayer steel, different steel plates are joint together to

*Corresponding author: Jun Ma Email address: zzulimajun@126.com

Accepted Manuscript Not Copyedited

form a layered structure by methods such as explosive welding [10], rolling [11], and braze [12]. Research in this field has been predominantly focused on fabrication and its effect to the mechanical properties and bonding interface quality. Kacar cladded 316L stainless steel-din-P355GH steel by explosive welding, in which the bond interface displayed a wavy morphology in the weld microstructure of microscopic observation [13]. The hardness of the cladded material increased near the bond interface and the toughness was significantly higher than that of the parent plate alone. Zamani prepared stainless steel/carbon steel coaxial pipes using the explosive welding method and studied the effect of explosive mass on the microstructure of the bonding interface of the layer structure [14]. Results demonstrated that the transition from wavy interface to smooth occurs with a decline in explosive load and grains near the interface were elongated along the explosive direction due to the high localized plastic deformation in metal collision. Jing boned SUS304 stainless steel and carbon steel by hot rolling [15]. The boding quality of the material was evaluated by the interfacial microstructures, composition diffusion and peeling fractographies. Results showed that many bonding dimples appeared on the peeling interface and the density increased with the rise of rolling pass, which can improve the bonding strength of the clad plate. Mousavi presented the interface microstructure evolutions of explosively welded cp-Titanium/AISI 304 stainless steel composites due to heat treatment [16]. The post heating temperatures and corresponding intermetallic product at the joint interface are provided in this research.

In recent years, titanium aluminide intermetallics have received increasing attention due to excellent performance properties, such as high melting point, high specific strength and stiffness, and good corrosion resistance [17-21]. Such characteristics mean Ti-Al intermetallic is a suitable prospect for high temperature structural materials. Three major intermetallic titanium aluminide alloys exist: TiAl, Ti_3Al, and Al_3Ti [22]. Among them, Al_3Ti intermetallic materials have the lowest density and highest Young's modulus, as well as favorable corrosive resistance properties and high-temperature creep resistance. However, the low fracture toughness of Al_3Ti alloys at room temperature has greatly limited their application [23,24]. Various researchers have attempted to improve the toughness of the intermetallics by fiber or particle reinforcement, however, the toughening effect has not been significant [25,26]. The excellent mechanical properties of shell has been discovered in recent years [27,28]. Shell is mainly composed of brittle calcium carbonate and microstructure observation shows it is formed by the regular lamination of wafers. When the shell is impacted by external forces, the cracks

Accepted Manuscript Not Copyedited

expand and deflect along the interface to improve the fracture toughness [29,30]. Thus, according to the special toughening principle of the shell structure, a new type of lightweight laminate composite material has been developed. The Ti/Al_3Ti metal/intermetallic (MIL) composite consists of alternative Ti and Al_3Ti layers, while the aluminide phases provide high hardness and strength to the composite. Additionally, titanium alloy provides the necessary high toughness and ductility [31,32].

A series of studies have been conducted on the fracture behavior and properties of Ti/Al_3Ti MIL composites. Adharapurapu et al. have studied the crack growth mechanism of laminate composites using single edge-notched bend specimens [1]. The results indicate that the toughness and fatigue resistance of monolithic Al_3Ti is improved by incorporating a ductile layer of Ti, and toughness is improved by an order of magnitude. Rohatgi et al. investigated the crack growth and toughening mechanisms of Ti/Al_3Ti laminate composites [2]. The study shows that the toughening mechanisms of Ti/Al_3Ti laminate composites involve crack deflection, crack bridging, stress redistribution, and crack front convolution. Peng et al. studied the mechanical properties and fracture behavior of fabricated laminated composites using the three-point bending test [33]. Non-catastrophic fracture behavior of the material was identified as a result of crack deflection along the interface. Meanwhile, extensive plastic deformation was identified in the Ti layers, which can also improve fracture toughness of the material during the bending process. Zhou et al. have developed a novel specimen to study the tensile behavior and fracture mechanism of Ti/Al_3Ti under quasi-static and high strain rates [34]. The research shows that the fracture only occurs in the interface under quasi-static tensile conditions, and the fracture of Ti alloy is determined to be quasi-cleavage failure mode under both conditions. Price et al. investigated the effect of residual Al at the intermetallic centerline on the strength and fracture toughness of the composite through the four-point bending test [35]. The results demonstrate that cracks always initiate in the intermetallic region, and rarely at the centerline. Researchers have also studied the fracture properties of Ti/Al_3Ti by different methods. However, no attention has been given to the reinforcing effects of the interface and near-interface zone on the fracture behavior of Al_3Ti. Fracture toughness, as an important parameter to predict the fracture properties of brittle materials, is suitable to evaluate the toughness of Al_3Ti intermetallic. Numerous methods have been developed to study fracture toughness, such as the single edge notched beam（SENB）[36], the double cantilever beam (DCB) [37], double-torsion (DT) [38], indentation strength in bending (ISB）[39], and indentation fracture method (IF) [40]. Compared with the other techniques which require a special specimen, the indentation method is

Accepted Manuscript Not Copyedited

much easier to carry out, as only a polished specimen and a microhardness tester is needed.

The objective of this work is to study the reinforcing mechanism and effect of the interface in the MIL composite on the fracture of Al_3Ti intermetallic. First, the Ti/Al_3Ti MIL composite is synthesized via reactive foil sintering in vacuum using titanium alloy and pure aluminum foils. The microstructure characterization of the composite is performed using scanning electron microscopy (SEM), and electron back-scattered diffraction (EBSD). The fracture toughness on different regions is studied by microhardness tester. In addition, the failure mode of the matrix layer, interface, and near-interface zone are investigated using SEM.

2. Experimental Procedures

2.1 Material fabrication

The Ti/Al_3Ti MIL composite was processed by reactive foil sintering in a vacuum. The Ti6Al4V alloy and 1060 aluminum foils were then stacked alternatively and reacted in a hot-pressing furnace. The design concept of the material system is schematically illustrated in Fig. 1. The thickness of the initial titanium alloy and Al foils was selected in such a state that all of the initial Al is consumed to form Al_3Ti with alternating Ti layers. The final sintering product took the form of alternate layers of Al_3Ti and residual titanium alloy.

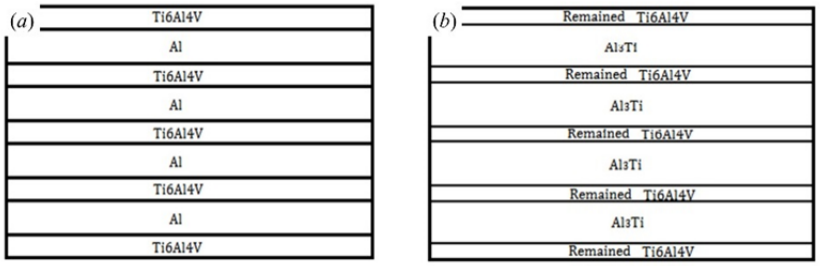

Fig. 1. A schematic vertical cross section of the Ti/Al_3Ti composite before and after reactive foil sintering process: (a)Before reactive foil sintering; (b)After reactive foil sintering.

2.2 Microstructure characterization

The specimens were cut from prepared materials by wire cut electrical discharge machine. All samples were then ground using 600, 1000, 1500, 2000 grit silicon carbide paper, respectively, and polished with Al_2O_3 polishing paste (the Al_2O_3 powder size is 0.5 μm) for microstructure observation. The microstructure characterization of Ti/Al_3Ti laminate composite was performed using a LEICA DVM6

Accepted Manuscript Not Copyedited

three-dimension microscope and Phenom Pro XL SEM. The phase distribution, grain size, and stress distribution of Ti/Al_3Ti laminate composite was investigated by electron back-scattered diffraction technique. To obtain the backscattered electron diffraction pattern of the Ti/Al_3Ti composite, stress-relief annealing was conducted on the composite to reduce internal stress in the material. The material was then treated in a heat treating furnace at 300°C for three hours before being cooled inside the furnace. Finally, the specimen was prepared by vibration polishing to ensure that there was no obvious height difference at the interface, so as to obtain high quality experimental data.

2.3 Experimental theory and procedure

Vickers microhardness at different locations of the Ti/Al_3Ti was measured using the Brinell hardness tester. The load applied for the hardness test was adjusted to generate cracks in the corner of the indentation, and the dimensions of the resulting indentation and crack were measured.

The effect of the interface on toughness was analyzed using the indentation fracture method [41]. The method is derived from the measurement procedure of the Vickers hardness test. Marshall and Lawn established a relationship between toughness (K_{IC}) and microhardness (H_V) which is detailed as follows [42]:

$$H_V = \frac{P}{\alpha a^2} \tag{1}$$

$$K_{IC} = \frac{P}{\beta c^{2E}} \tag{2}$$

where α , β are constants, P is the load applied on the indenter, a is the half diagonal of the indentation, c is the half length of the crack corresponding to the applied load, and E is Young's modulus.

According to Marshall and Lawn, the residual stress does not contribute a specific factor to the fracture toughness, but instead affects the length 2c of the cracks (see Fig. 2).

Accepted Manuscript Not Copyedited

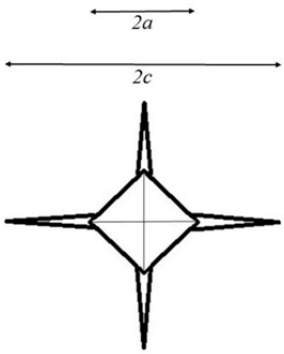

Fig. 2. Cracks around hardness indentation.

Numerous modifications have been made regarding this result [43-48], in which scholars have developed a number of equations to calculate K_{IC}. The value of fracture toughness K_{IC} can be calculated by the length of the cracks growing in the corners of the Vickers indentation, and the equations proposed by Evans and Niihara are most widely used.

$$K_{IC}=0.16\left(\frac{c}{a}\right)^{-1.5} Ha^{\frac{1}{2}} \quad \text{(Evans \& Charles)} \quad (3)$$

where,

$$H_V=1.8\frac{P}{a^2} \quad (4)$$

$$K_{IC}=0.067\left(\frac{E}{H_V}\right)H_V\alpha^{0.5}\left(\frac{c}{a}\right)^{-1.5} \quad \text{(Niihara)} \quad (5)$$

The toughening results of the interface, as well as fracture toughness on the regions of Al_3Ti layer, interface, and near-interface is calculated by the same equation. In this study, the fracture toughness is determined by Eq. (3). It has no relation to the Young's modulus, because the Young's modulus at different locations of the laminate composite can vary greatly. The half average length of the diagonal (a), and the average length of the cracks (c) obtained in the tip of the Vickers marks were recorded during the test to calculate the fracture toughness (K_{IC}). The two parameters mentioned above are shown in Fig. 3.

Accepted Manuscript Not Copyedited

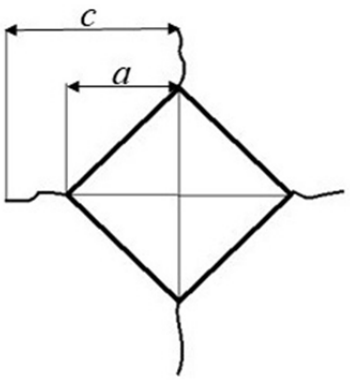

Fig. 3. Vickers indentation mark.

3. Result and Discussion

3.1 Microstructure observation

The microstructure of the Ti/Al_3Ti laminate composite, including Ti layers (light regions) and formed Al_3Ti layers (dark regions), is provided in Fig. 4. It can be seen that bonding at the interface is good, but there are many discontinuous black lines in the center of the Al_3Ti layers. The formation of the intermetallic centerline is related to the reaction mechanism [49]. In the fabrication process, the reaction temperature is higher than the melting point of Al, and the existence of molten Al allows reacting Al_3Ti to move away from the Ti layer. Thus, a continuous reaction interface is maintained. When the reaction interface migrating away from one Ti layer meets its reciprocal moving downward from the next layer, the migration ends and the oxides at each front come together to form the intermetallic centerline. The centerline can be controlled by initial foil preparation (oxide removal), foil composition and purity, and foil thickness.

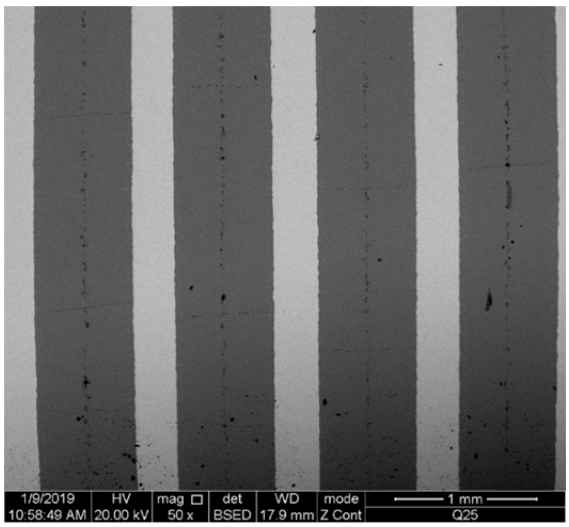

Accepted Manuscript Not Copyedited

Fig. 4. Microstructure of the prepared Ti/Al_3Ti laminate composite.

3.2 Electron backscattering diffraction

The EBDS results around the interface of Ti/Al_3Ti composite are illustrated in Fig. 5. As can be seen from the diffraction contrast diagram shown in Fig. 5(a), the calibration rate is adequately high, indicating that the data results of EBSD testing are reliable. The results demonstrate that the Ti and Al_3Ti layer are both single phase. The corresponding phase distribution of the composite is provided in Fig. 5(b), in which the blue indicates Al_3Ti, and the red represents Ti. The invalid data area in the phase mapping is marked in white. High stress on the interface causes the grain to deform severely, leading to invalid diffraction data for this area. Furthermore, there is a small intergranular space in the coarse grain, and data results are unavailable in this area which also contributes to the failure of the diffraction pattern.

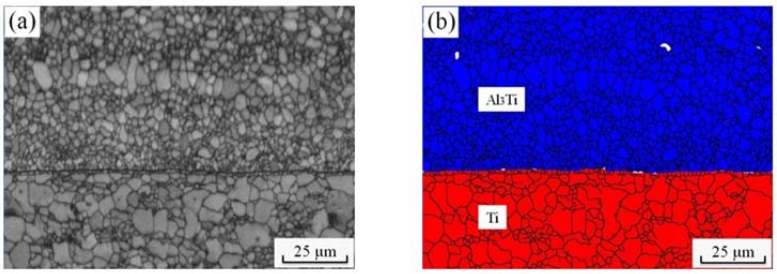

Fig. 5. Results of EBSD analysis of Ti/Al_3Ti: (a) Diffraction contrast image; (b) Phase distribution.

From the EBDS results of the laminate composite, it can be determined that the size of the grains in different locations of the Al_3Ti matrix varies greatly, and the father apart the interface, the bigger the size. This is because the reaction begins at the interface, and the molten Al allows reacting Al_3Ti to move away from the interface. The formation of the grain of the Al_3Ti intermetallic undergoes nucleation and growth. The closer the grain to the interface, the later it appears, and the less time for its growth. Accordingly, the grains near the interface is smaller. Every reactive Al_3Ti layer can be divided by grain size into three regions: fine grain zone, coarse grain zone and interface zone, the thicknesses of which are 25 μm, 7 μm, and 1 μm, respectively.

Accepted Manuscript Copyedited

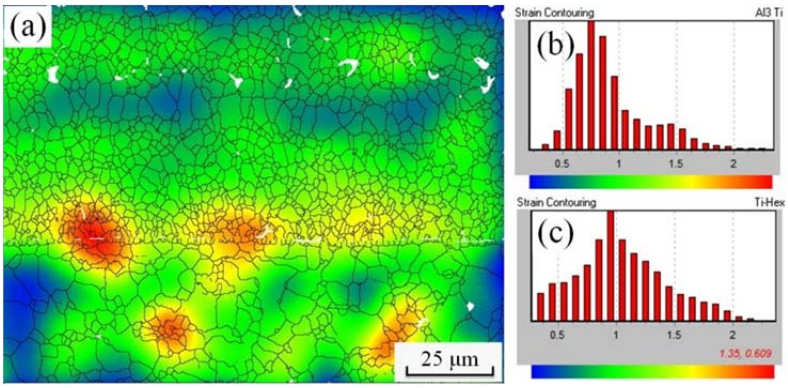

Fig. 6. Stress distribution of Ti/Al_3Ti MIL composites: (a) Stress distribution; (b) Strain statistics of Al_3Ti; (c) Strain statistics of Ti.

The distribution of internal stress around the interface of the Ti/Al_3Ti laminate composite is given in Fig. 6. It can be observed that the stress in the interface is the maximum, and there is an area with obvious stress concentration in the Ti layer. In addition, the grains in the stress concentration area are all very tiny. The stress concentration in the Ti layer is caused by the original deformation in the raw titanium foils While the stress concentration at the interface can be attributed to the difference of coefficient of thermal expansion between Ti and Al_3Ti. The thermal expansion coefficient is 8.5×10^{-6} /°C for Ti, and 13×10^{-6} /°C for Al_3Ti. Due to the temperature changes during fabrication, the layer of Ti resists compressive stress, while the layers of Al_3Ti bear tensile stress. Therefore, there is large residual stress at the interface between the different layers. The introduced stress due to the difference of the thermal expansion coefficient has a relationship with the thickness of the foil, temperature history, and sintering pressure during preparation.

3.3 Indentation experiments

（1）Al_3Ti layer

The force applied by the microhardness tester head in the indentation experiment was 1 KN, and there are some obvious cracks in the corners of the indentation under this load. The typical crack distribution in the Al_3Ti layers is provided in Fig. 7(a).

Accepted Manuscript Not Copyedited

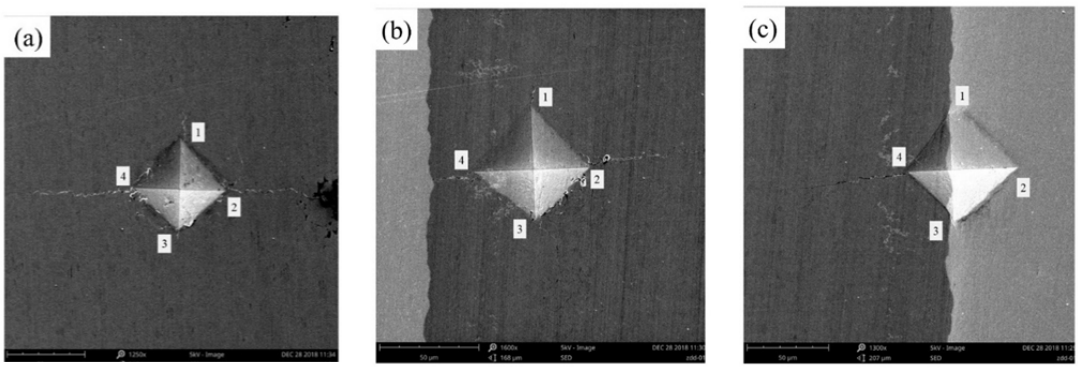

Fig. 7 Indentation and crack distribution: (a) in the Al_3Ti layer, (b)near the interface, (c) at the interface.

Table 1. Data results of indentation test for Al_3Ti intermetallic layer

	d_1 (μm)	d_2 (μm)	a (μm)	c (μm)	K_{IC}(MPa$\sqrt{m}$)
No.1	56.74	55.22	27.99	68.18	5.01
No.2	66.79	67.42	33.55	65.96	5.27
No.3	60.34	59.62	29.99	74.64	4.38
No.4	59.81	58.31	29.53	65.67	5.03
No.5	58.43	58.42	29.21	65.96	5.27
Average	60.12	60.10	30.05	68.08	4.99

The material crushing around the indentation of the Al_3Ti illustrated in Fig. 7(a), is due to the brittle characteristics of Al_3Ti intermetallic. The cracks generate in three corners of the indentation, and expand along the radial direction. The propagation directions of the cracks initiated in corner 2 and corner 4 are both parallel to the laminate, and the other crack growth orientations are perpendicular to the laminate. It is obvious that the crack length is much longer for those parallel to the laminate compared to the perpendicular ones. This is because the laminate material has a good homogeneous structure and superior performance along the laminate direction compared to the other. By measuring the length of the diagonal indentation (d_1 and d_2) and cracks, the results of the indentation test for Al_3Ti intermetallic are provided in Table 1.

(2) Near-interface

Figure 7(b) shows a typical crack distribution near the interface. Three radial cracks can be observed, as well as many tiny circumferential cracks around the indentation. The crack length in the direction perpendicular to the laminate is also longer than the parallel one. The crack initiated in corner 4

Accepted Manuscript Not Copyedited

propagates toward to the interface, and ceases to extend when it reaches the interface, due to the high toughness of the Ti layer. No cracks in the next layer of Ti are found. For this reason, the crack length in this corner is much shorter than the corresponding one in the Al_3Ti, and the calculated fracture toughness will be correspondingly higher, as seen in the data provided in Table 2.

Table 2. Data results of indentation test near the interface

	d_1 (μm)	d_2 (μm)	a (μm)	c (μm)	K_{IC}(MPa$\sqrt{m}$)
No.1	60.75	61	30.44	51.38	7.66
No.2	60.75	59.84	30.15	47.23	8.70
No.3	60.98	61	30.50	50.52	7.86
No.4	60.98	61	30.50	46.67	8.85
No.5	60.06	60.31	30.09	48.46	8.37
Average	60.70	60.63	30.34	48.85	8.29

(3) Interface

For the indentation fracture test on the interface, one diagonal line of the indentation coincides with the interface, as shown in Fig. 7(c). The shape of the indentation is not a standard rhombus, and there is only one crack in all four corners, which is on the Al_3Ti layer. For the other three corners located in the interface and Ti layer, no cracks or other defects occur. The indentation size, crack length, and calculated fracture toughness in the test are given in Table 3.

Table 3. Data results of indentation test at the interface

	d_1 (μm)	d_2 (μm)	a (μm)	c (μm)	K_{IC}(MPa$\sqrt{m}$)
No.1	67.18	66.15	33.33	45.13	9.31
No.2	66.27	67.27	33.39	40.48	10.96
No.3	72.25	68.19	35.11	41.61	10.52
No.4	69.49	67.73	34.31	44.34	9.56
No.5	67.88	66.8	33.67	42.53	10.18
Average	68.61	67.23	33.96	42.82	10.11

3.4 Discussion

It can be seen from the indentation shape and crack distribution in the Al_3Ti layers, near-interface zone,

Accepted Manuscript Not Copyedited

and interface (as illustrated in Fig. 7(a), Fig. 7(b), and Fig. 7(c), respectively), that the indentation in the Al_3Ti layer is similar to the one in the near-interface zone, as well as the crack propagation path. The radial cracks in these two zones are found to be almost the same in length, expect for corner 4. This is because there is a distance between the indentation in the Al_3Ti layer and the near-interface zone, and it has no additional effect on crack propagation for the interface. In the near-interface zone, it is clear that the crack initiated in corner 4 stops propagating when reaching the interface due to the higher toughness of the titanium alloy in the next layer. Two major extrinsic toughness mechanisms exist in this layer. One is crack blunting, which occurs when the crack encounters the metal layer and is blunted. A significant amount of energy is required for the crack to re-nucleate, however, the residual energy here is too small to re-nucleate, and the crack stop growing. The other toughness mechanism is the crack front convolution, which occurs in the laminated structure consisting of phases with different ductility. When the crack front grows from the brittle intermetallic layer to the metal layer with higher ductility, it becomes highly convoluted, and the crack growth is restricted by the plastic deformation.

There is a big difference between the shapes of indentations located in the interface and the other two zones. This is because one half of the indentation occurs in the Al_3Ti layer and other half presses above the Ti layer. The hardness of Al_3Ti intermetallic is 516 Hv, which is much higher than the 330 Hv of the Ti alloy. This variation creates an irregular rhombus for the indentation on the interface. The crack only appears in a corner located in the Al_3Ti layer, and no cracks are found in the other three corners of the indentation due to the high toughness of the Ti alloy. For this reason, the crack has less average length, thus the calculated fracture toughness of the interface when using the average crack length will be higher than the other two zones.

Figure 8 illustrates an interesting phenomenon that is observed in the cracks near the interface. Under these conditions, cracks along the diagonals parallel to the interface propagate close to the interface. One possible reason for this is that residual stress near the interface is higher than in the other area, just like the internal stress distribution of the EBDS result shown in Fig. 6. The residual stress increases the driving force for crack propagation, and cracks tend to grow and spread to this area.

Accepted Manuscript Not Copyedited

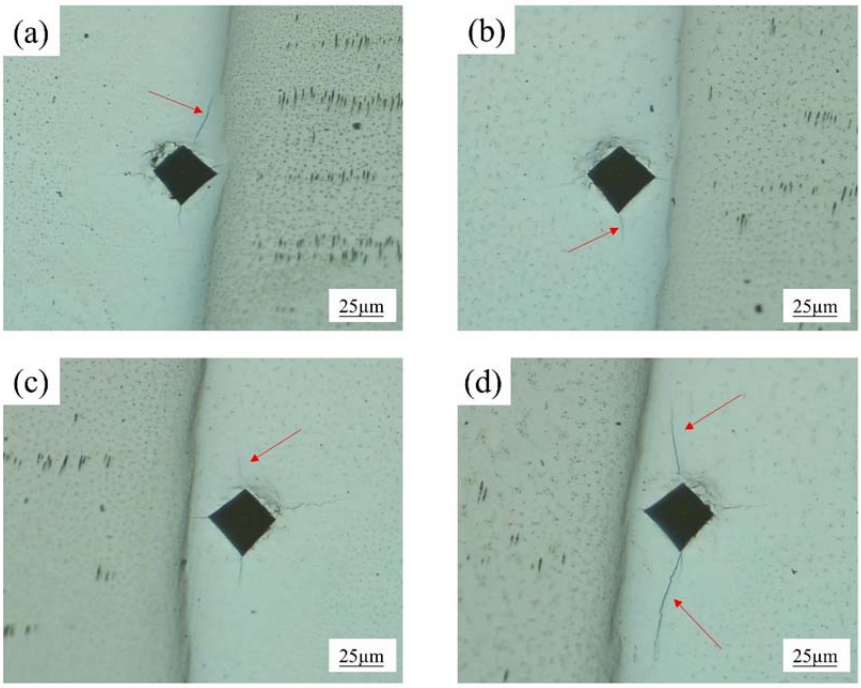

Fig. 8. Growing path for cracks near the interface, which decline toward to the interface.

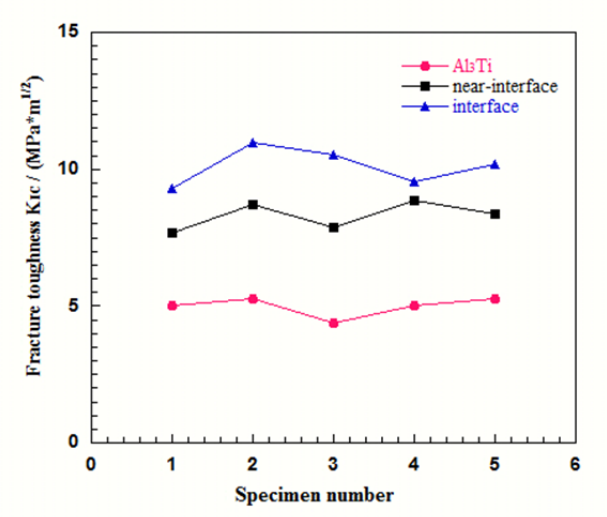

Fig. 9. Fracture toughness for different zones of Ti/Al_3Ti laminate composite.

The K_{IC} for the different zones of Ti/Al_3Ti is shown in Fig. 9. The value of K_{IC} fluctuates less with changes to the same zone, illustrating that the reaction is uniform during the preparing process, and the product has a dense structure and homogeneous properties. However, the fracture toughness shows a large variation among the three zones. The interface zone has the highest fracture toughness, followed by the near-interface zone, and Al_3Ti matrix has the lowest fracture toughness. The average fracture toughness at the Al_3Ti layer is 4.99 $MPa\sqrt{m}$, and it will increase as it gets closer to the interface. The increase to near-interface value is 8.29 $MPa\sqrt{m}$, finally reaching 10.11 $MPa\sqrt{m}$. This result indicates

that laminate ductile reinforcements in brittle intermetallic improves resistance to crack propagation by more than twice that of Al_3Ti.

4. Conclusion

In this paper, Ti/Al_3Ti metal/intermetallic laminate composite was successfully synthesized by reactive sintering in a vacuum using Ti6Al4V and Al foils under the controls of temperature and pressure. Microstructure and internal stress were analyzed by SEM and EBDS. Micro fracture toughness on the microscopic scale was then studied using a microhardness tester. The following conclusions can be drawn from this work:

(1) The Al foils were entirely consumed by the Ti6Al4V to form Al_3Ti during the sintering process. The EBDS results demonstrate that the final product is composited by alternate layers of Al_3Ti and the residual titanium alloy.

(2) When the initial Al and Ti6Al4V foils were heated or cooled during sintering, remnant stress was caused to the microstructure and properties of the laminate composite due to their various expansion coefficients. The internal stress distribution measured by EBDS shows that there was a high level of stress at the interface, which made the grains at this area very small.

(3) Under the two mechanisms of crack blunting and crack front convolution, the crack initiated at the corner of the Vickers indentation was prevented from propagation by the interface. The cracks near the interface tended to propagate towards the interface due to the effect of internal stress and grain size.

(4) The metal layers improved the toughness of the Al_3Ti intermetallic，and the effect increased correspondingly to a decrease of distance between the interface. The fracture toughness at the interface was determined to be more than twice the value of the Al_3Ti matrix.

Accepted Manuscript Not Copyedited

Acknowledgements

The authors gratefully acknowledge the financial supports of this study by the National Natural Science Foundation of China (No.11602230), Program for Innovative Research Team in Science and Technology in University of Henan Province (18IRTSTHN015), Key Scientific Projects of University in Henan Province (20B430021).

References

[1] R.R Adharapurapu, K.S Vecchio, F Jiang, and A Rohatgi, Effects of ductile laminate thickness, volume fraction, and orientation on fatigue-crack propagation in Ti-Al3Ti metal-intermetallic laminate composites, *Metall. Mater. Trans. A.*, 36(2005), No. 6, p.1595.

[2] A Rohatgi, D.J Harach, K.S Vecchio, and K.P Harvey, Resistance-curve and fracture behavior of Ti-AlTi metallic–intermetallic laminate (MIL) composites, *Acta. Mater.*, 51(2003), No. 10, p. 2933.

[3] M Tayyebi and B Eghbali, Microstructure and mechanical properties of SiC-particle-strengthening tri-metal Al/Cu/Ni composite produced by accumulative roll bonding process, *Int. J. Miner. Metall. Mater.*, 25(2018), No. 3, p.357.

[4] O Emadinia, S Simões, F Viana, and M.F Vieira, Ni/Ti and Ni/Al Laminated Composites Produced by ARB and Annealing: Microstructural Aspects, *Microsc. Microanal.*, 21(2015), No. S5, p. 23.

[5] I Okulov, U Kuhn, T Marr, and J Freudenberger, Deformation and fracture behavior of composite structured Ti-Nb-Al-Co(-Ni) alloys, *Appl. Phys. Lett.*, 104(2014), No. 7, p. 1085.

[6] R Jafari and B Eghbali, Study on the reaction mechanism and intermetallic compound formation in tri-metal Ti/Al/Nb composite, *J. Alloy. Compd.*, 741(2018), p. 1030.

[7] M Hojo, N Iwasaki, F Sekino, and O Shojiro, Fracture behavior under fatigue loading at room temperature and its influence on critical current of Nb-Ti/Cu composite wire, *Cryogenics*, 29(2006), No. 39, p. 627.

[8] N Kahraman and B.S Gulenc, Microstructural and mechanical properties of Cu–Ti plates bonded through explosive welding process, *J. Mater. Process. Tech.*, 169(2005), No. 1, p. 67.

[9] B.X Liu, L Geng, X.L Dai, F.X Yin, and L.J Huang, Multiple Toughening Mechanisms of Laminated Ti-TiBw/Ti Composites Fabricated by Diffusion Welding, *Metall. Mater. Trans. A.*, 848(2016), p. 196.

[10] N.V Rao and G.M Reddy, Structure and Properties of Explosive Clad HSLA Steel with Titanium, *T. Indian. I. Metals.*, 67(2014), No. 1, p. 67.

[11] Kim, In-Kyu, and S.I Hong, Roll-Bonded Tri-Layered Mg/Al/Stainless Steel Clad Composites and their Deformation and Fracture Behavior, *Metall. Mater. Trans. A.*, 44(2013), No. 8, p. 3890.

[12] W Jiang, J Gong, and S.T Tu, A new cooling method for vacuum brazing of a stainless steel plate–fin structure, *Mater. Design.*, 31(2010), No. 1, p. 648.

[13] R Kacar and M Acarer, An investigation on the explosive cladding of 316L stainless steel-din-P355GH steel, *J. Mater. Process. Tech.*, 152(2004), No. 1, p. 91.

Accepted Manuscript Not Copyedited

[14] E Zamani and G.H Liaghat, Explosive welding of stainless steel–carbon steel coaxial pipes, *J. Mater. Sci.*, 47(2012), No. 2, p. 685.

[15] Y Jing, Y Qin, X Zang, and Y Li, The bonding properties and interfacial morphologies of clad plate prepared by multiple passes hot rolling in a protective atmosphere, *J. Mater. Process. Tech.*, 214(2014), No. 8, p. 1686.

[16] S.A.A.A Mousavi and P.F Sartangi, Effect of post-weld heat treatment on the interface microstructure of explosively welded titanium–stainless steel composite, *Mat. Sci. Eng. A*, 494(2008), No. 1, p. 329.

[17] J Soyama, M Oehring, T Ebel, K.U Kainer, and F Pyczak, Sintering Behavior and Microstructure Formation of Titanium Aluminide Alloys Processed by Metal Injection Molding, *JOM*, 69(2017), No. 4, p. 676.

[18] Y Cao, N Wei, X Han, C Guo, J Du, W He, J Ma and F Jiang, Mechanical response of titanium tri-aluminide intermetallic alloy, *Mat. Sci. Eng. A*, 706(2017), p. 242.

[19] G.P Chaudhari and V.L Acoff, Titanium aluminide sheets made using roll bonding and reaction annealing, *Intermetallics*, 18(2010), No. 4, p. 472.

[20] Y.Y Chen, Y Jia, S.L Xiao, J Tian, and L.J Xu, Review of the Investment Casting of TiAl Based Intermetallic Alloys, *Mater. China.*, 49(2010), No. 11, p. 1281.

[21] D.X Wei, Y Koizumi, M Nagasako, and A Chiba, Refinement of lamellar structures in Ti-Al alloy, *Acta. Mater.*, 152(2017), p. 81.

[22] M Konieczny, Relations between Microstructure and Mechanical Properties in Laminated Ti-Intermetallic Composites Synthesized Using Ti and Al Foils, *Key Eng. Mater.*, 592(2014), No. 12, p. 728.

[23] T.E.J Edwards, F.D Gioacchino, G Mohanty, J Wehrs, J Michler, and W.J Clegg, Longitudinal twinning in a TiAl alloy at high temperature by in situ micro-compression, *Acta. Mater.*, 148(2018), p. 202.

[24] B.B Yu, H Yan, Q.J Wu, Z Hu, and F.H Chen, Microstructure and corrosion behavior of Al3Ti /ADC12 composite modified with Sr, *Int. J. Miner. Metall. Mater.*, 25(2018), No. 7, p. 840.

[25] Y Han, C Lin, X Han, Y Chang, C Guo, and F Jiang, Fabrication, interfacial characterization and mechanical properties of continuous Al2O3 ceramic fiber reinforced Ti/Al3Ti metal-intermetallic laminated (CCFR-MIL) composite, *Mat. Sci. Eng. A.*, 688(2017), p. 338.

Accepted Manuscript Not Copyedited

[26] M.J Wang, H Hao, L Hu, S.M Zhang. W Mao, S Cheng, and P Feng, Microstructure and interfacial strength of SiC fiber-reinforced Ti17 alloy composites with different consolidation temperatures, *Rare Metals*, 9(2018), p. 1.

[27] H Kakisawa and T Sumitomo, The toughening mechanism of nacre and structural materials inspired by nacre, *Sci. Technol. Adv. Mater.*, 12(2011), No. 6.

[28] B Gludovatz, F Walsh, E.A Zimmermann, S.E Naleway, R.O Ritchie, and J.J Kruzic, Multiscale structure and damage tolerance of coconut shells, *J. Mech. Behav. Biomedi.*, 76(2017), p. 76.

[29] M.A Meyers and P.Y Chen, Structural biological materials: critical mechanics-materials connections, *Science*, 339(2013), No. 6121, p. 773.

[30] M O"Neill, D Cafiso, R Mala, G.L Rosa, and D Taylor, Fracture toughness and damage development in limpet shells, *Theor. Appl. Fract. Mec.*, 96(2018), p. 168.

[31] K.S Vecchio and F Jiang, Fracture toughness of Ceramic-Fiber-Reinforced Metallic-Intermetallic-Laminate (CFR-MIL) composites, *Mat. Sci. Eng. A.*, 649(2016), p. 407.

[32] L Zhang, B.L Wu, and Y.L Liu, Microstructure and mechanical properties of a hot-extruded Al-based composite reinforced with core-shell-structured Ti/Al3Ti, *Int. J. Miner. Metall. Mater.*, 24(2017), No. 12, p. 1431.

[33] L.M Peng, H Li, and J.H Wang, Processing and mechanical behavior of laminated titanium-titanium tri-aluminide (Ti-Al3Ti) composites, *Mat. Sci. Eng. A.*, 406(2005), No. 1, p. 309.

[34] P Zhou, C Guo, E Wang, Z Wang, C Ye, and F Jiang, Interface tensile and fracture behavior of the Ti/Al3Ti Metal-Intermetallic Laminate (MIL) composite under quasi-static and high strain rates, *Mat. Sci. Eng. A.*, 665(2016), p. 66.

[35] R.D Price, F Jiang, R.M Kulin, and K.S Vecchio, Effects of ductile phase volume fraction on the mechanical properties of Ti-Al3Ti metal-intermetallic laminate (MIL) composites, *Mat. Sci. Eng. A.*, 528(2010), No. 7, p. 3134.

[36] D Damjanović, D Kozak, Y Matvienko, and N Gubeljak, Correlation of Pipe Ring Notched Bend (PRNB) specimen and Single Edge Notch Bend (SENB) specimen in determination of fracture toughness of pipe material, *Fatigue. Fract. Eng. M.*, 40(2017), No. 8, p. 1251.

[37] F Sacchetti, W.J.B Grouve, L.L Warnet, and V.I Fernandez. Interlaminar fracture toughness of 5HS Carbon/PEEK laminates. A comparison between DCB, ELS and mandrel peel tests, *Polym*

Accepted Manuscript Not Copyedited

Test, 66(2018), p. 13.

[38] J.A Wang and T Tan, A method for evaluating the fatigue crack growth in spiral notch torsion fracture toughness test, Arch Appl Mech, 89(2019), No. 5, p. 813.

[39] P Chantikul, G.R Anstis, B.R Lawn, and D.B Marshall, A Critical Evaluation of Indentation Techniques for Measuring Fracture Toughness, Part II, Strength Method, *J. Am. Ceram. Soc.*, 64(2010), No. 9, p. 539.

[40] L Sun, D Ma, L Wang, X Shi, J Wang, and W Chen, Determining indentation fracture toughness of ceramics by finite element method using virtual crack closure technique, *Eng. Fract. Mech.*, 197(2018), p. 151.

[41] D Chicot, A Pertuz, F Roudet, M.H Staia, and J Lesage, New developments for fracture toughness determination by Vickers indentation, *Met. Sci. J.*, 20(2004), p. 877.

[42] D.B Marshall and B.R Lawn, Indentation of brittle Materials, *ASTM*, 889(1986), p. 26.

[43]A.G Evans and E.A Charles, Fracture Toughness Determination by Indentation, *J. Am. Ceram. Soc.*, 59(1976), No. 7, p. 371.

[44] M.T Laugier, New formula for indentation toughness in ceramics, *J. Mater. Sci. Lett.*, 6(1987), No. 3, p. 355.

[45] J.J Kruzic and R.O Ritchie, Determining the toughness of ceramics from vickers indentations using the crack-opening displacements: an experimental study, *J. Am. Ceram. Soc.*, 86(2003), No. 8, p. 1433.

[46] Y Feng, T Zhang, and R Yang, A Work Approach to Determine Vickers Indentation Fracture Toughness, *J. Ame. Ceram. Soc.*, 94(2011), No. 2, p. 332.

[47] J Gong. Determining indentation toughness by incorporating true hardness into fracture mechanics equations, *J. Eur. Ceram. Soc.*, 19(1999), No. 8, p. 1585.

[48] D Ma, S Liang, T Gao, J Wang and L Wang, New method for extracting fracture toughness of ceramic materials by instrumented indentation test with Berkovich indenter, *J. Eur. Ceram. Soc.*, 37(2017), No. 6, p. 2537.

[49] D.J Harach and K.S Vecchio, Microstructure evolution in metal-intermetallic laminate (MIL) composites synthesized by reactive foil sintering in air, *Metall. Mater. Trans. A.*, 32 (2001), No. 6, p.1493.

Accepted Manuscript Not Copyedited

中图分类号 **TB331**　　二级学科名称 **材料学**

Accepted Manuscript Not Copyedited